Dynamic hydrological modeling in drylands with TRMM based rainfall

Article

Published Version

It is advisable to refer to the publisher's version if you intend to cite from the work.

www.reading.ac.uk/centaur

CentAUR

Central Archive at the University of Reading

Article

Dynamic Hydrological Modeling in Drylands with TRMM Based Rainfall

Elena Tarnavsky [1],*, Mark Mulligan [2], Mohamed Ouessar [3], Abdoulaye Faye [4] and Emily Black [1]

[1] Meteorology Department, University of Reading, Earley Gate, POBox 243, Reading RG6 6BB, UK;
E-Mail: e.c.l.black@reading.ac.uk

[2] Geography Department, King's College London, The Strand, London WC2R 2LS, UK;
E-Mail: mark.mulligan@kcl.ac.uk

[3] Institut des Régions Arides (IRA), Médenine 4119, Tunisia; E-Mail: ouessar@yahoo.com

[4] Centre des Suivi Ecologique (CSE), Fann Résidence, Dakar, B.P. 15532, Senegal;
E-Mail: aboufaye@cse.sn

* Author to whom correspondence should be addressed; E-Mail: e.tarnavsky@reading.ac.uk;
Tel.: +44-118-378-6020; Fax: +44-118-378-8905.

Abstract: This paper introduces and evaluates DryMOD, a dynamic water balance model of the key hydrological process in drylands that is based on free, public-domain datasets. The rainfall model of DryMOD makes optimal use of spatially disaggregated Tropical Rainfall Measuring Mission (TRMM) datasets to simulate hourly rainfall intensities at a spatial resolution of 1-km. Regional-scale applications of the model in seasonal catchments in Tunisia and Senegal characterize runoff and soil moisture distribution and dynamics in response to varying rainfall data inputs and soil properties. The results highlight the need for hourly-based rainfall simulation and for correcting TRMM 3B42 rainfall intensities for the fractional cover of rainfall (FCR). Without FCR correction and disaggregation to 1 km, TRMM 3B42 based rainfall intensities are too low to generate surface runoff and to induce substantial changes to soil moisture storage. The outcomes from the sensitivity analysis show that topsoil porosity is the most important soil property for simulation of runoff and soil moisture. Thus, we demonstrate the benefit of hydrological investigations at a scale, for which reliable information on soil profile characteristics exists and which is sufficiently fine to account for the heterogeneities of these. Where such information is available, application of DryMOD can assist in the spatial and temporal planning of water harvesting

according to runoff-generating areas and the runoff ratio, as well as in the optimization of agricultural activities based on realistic representation of soil moisture conditions.

Keywords: TRMM; drylands; Africa; rainfall; runoff; soil moisture; runoff harvesting

1. Introduction: Motivation and Objectives

Dryland regions are prone to desertification processes that are triggered by surface and soil water deficits. Thus, regional-scale management of water resources in drylands requires detailed information on water available as surface runoff and soil moisture over large heterogeneous landscapes. Plot-scale studies are representative of a relatively limited spatial heterogeneity and temporal variability that is effectively limited by highly variable and ephemeral hydrological fluxes [1]. A range of such experiments was carried out across the Mediterranean region, under the European projects EFEDA (European Field Experiment in Desertification-threatened Areas) and MEDALUS (Mediterranean Desertification And Land Use) [2], which led to a sequence of plot-scale modeling studies [3]. Large-scale hydro-climatologic modeling, on the other hand, usefully characterizes climate variability, including spatial and temporal patterns of rainfall, but fails to capture the complexity of hydrological fluxes in response to heterogeneity in soil properties at the regional scale, at which desertification processes operate and water resource management decisions are made [4,5].

The gap in scope, complexity, and scale between plot- and large-scale remote sensing and modeling techniques is addressed here through a new, purpose-built model, DryMOD. DryMOD is developed to bridge the scale-gap between fine- (~30 m spatial resolution) and coarse-scale (~8 km spatial resolution) models and is implemented within the framework of DeSurvey, one of the European Commission's integrated projects on desertification [6]. The regional spatial-scale, at which DryMOD operates, is directly relevant to policy decisions on rainwater harvesting and agricultural water management activities.

DryMOD is a remote sensing based dynamic model of the dryland water balance. DryMOD aims to provide (a) regional-scale maps of surface runoff generating areas and soil moisture stores and (b) an effective means of interpreting remote sensing data for policy-relevant decision support. In order to achieve these aims, DryMOD is a spatially distributed (grid based) model, which represents the processes that are most relevant to the onset of desertification, namely rainfall-runoff generation and changes in soil moisture due to infiltration of rainfall in the soil profile. Rainfall, evapotranspiration, infiltration, groundwater recharge, and runoff, as well as soil moisture distribution—the key hydrological fluxes—are estimated for each grid throughout a study region (Figure 1).

In DryMOD, the representation of the key processes and variables is based on improved spatial and temporal detail from free, public-domain remote sensing data. Specifically, this study builds on the novel method for rainfall intensity correction and spatial disaggregation of satellite-based rainfall estimates, which combines a coarse spatial but high temporal resolution dataset (providing information on rainfall intensity) and a coarse temporal but relatively high spatial resolution dataset (providing information on rainfall totals) [7]. Both datasets are based on rainfall retrievals from the Tropical Rainfall Measurement Mission (TRMM) sensor, and are used to provide the rainfall forcing for

DryMOD in raw form (non-corrected time-series) and as time-series corrected for the fractional cover of rainfall (FCR) at finer than 0.25 spatial resolution [7]. Here, we evaluate the DryMOD model at two pilot study regions in the belts north and south of the Sahara desert, respectively. As well as providing specific regional insight, we use DryMOD to explore the sensitivities of simulated runoff and soil moisture to the heterogeneity of soil parameters and to rainfall time-series with and without the fractional cover of rainfall (FCR) correction, and demonstrate the hydrological importance of applying the FCR-corrected time-series.

Figure 1. Schematic diagram of the soil profile and the processes represented in the DryMOD water balance model.
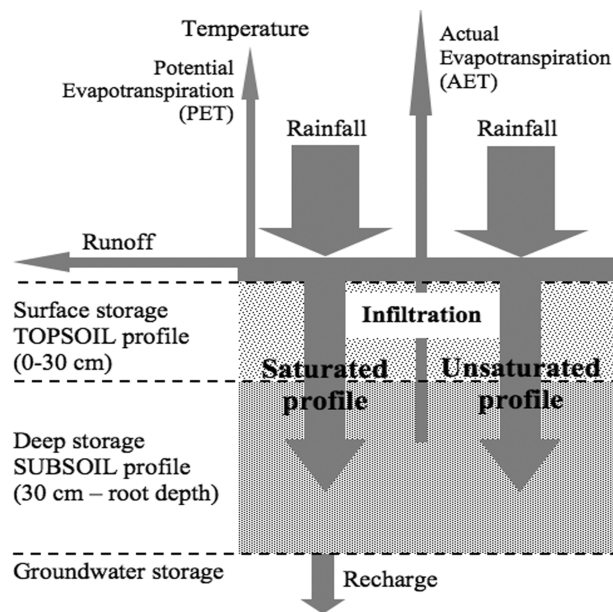
2. Background and Rationale

2.1. Description of the DryMOD Model: Spatial and Temporal Scales

DryMOD uses a grid cell representation of the study region with spatial resolution of 1 km, as determined by the spatial resolution of the available rainfall time-series, temperature climatology, and soil parameter databases used in the model. The 1-km spatial resolution is relevant to the spatial scale, at which rainfall generation processes operate. Rainfall in drylands is associated with cumulus convection systems, which operate at spatial scales of approximately 1 km and sub-daily temporal scales, while frontal systems are associated with scales exceeding 1,000 km and more than a day [8]. The importance of representing the spatial variability of rainfall (specifically convective rainfall) for hydrological modeling at resolutions below 2 km has been demonstrated in previous work in dryland catchments [8–11].

The spatial extent of the model is determined according to the boundaries of the study regions, which are defined following standard procedures for hydrological catchment delineation [12]. While runoff routing is not explicitly considered in DryMOD, modeling is still relevant at the hydrological catchment scale as the aim is to identify runoff-generating areas within a catchment and

to assess seasonal variability of runoff generation, the runoff ratio, and soil moisture stores. This information is valuable for effective planning of water harvesting and agricultural activities in water-limited environments.

A wealth of data allows for running hydrological models with daily to monthly time steps. However, representation of rainfall variability (specifically convective rainfall dominant in summer months in drylands) requires sub-daily temporal resolution for accurate partitioning of rainfall into infiltration and runoff [8]. Sub-daily information on rainfall is only available from remote sensing datasets, with spatial resolutions coarser than 1 km, and from some ground weather stations but generally not free of charge. Thus, DryMOD is designed with rainfall forcing at the required spatial and temporal resolutions from intensity corrected and spatially disaggregated TRMM-based rainfall forcing time-series generated from free, public-domain datasets [7].

The temporal coverage of the model is constrained only by the availability of historical data, *i.e.*, the 1998–2006 TRMM based rainfall datasets, which drive the rainfall simulation model [13,14]. Monthly outputs are generated automatically as part of the model applications in the pilot study regions.

2.2. Catchment-Based Modeling of Water Balance in Drylands with DryMOD

The water balance in DryMOD follows a general soil moisture budget approach, in which soil moisture storage is derived from rainfall as the main water input, and runoff, infiltration, evapotranspiration, and groundwater recharge as the key water "loss" components. Rainfall, temperature, and the hydraulic properties of soils play a key role in the water balance as the main controls of surface runoff dynamics, and the rates of infiltration and groundwater recharge, and ultimately determine soil moisture distribution. In DryMOD, rainfall reaching the surface is partitioned into infiltration and runoff, temperature is used to derive potential evapotranspiration (PET), and soil databases are used to derive soil hydraulic parameters in order to estimate soil moisture storage in the root zone for each 1-km grid over a given simulation period. In general form, the water balance equation at a point for time t can be written as:

$$\Delta SM = I - ET - GWR \tag{1}$$

where ΔSM is change in soil moisture storage, I is infiltration (vertical flow of rainfall into the root zone), ET is evapotranspiration (water loss from the soil profile), and GWR is groundwater recharge or drainage (vertical flow beyond the root zone layer). Currently, in DryMOD, leaf interception and water inputs from irrigation and runon contributions of water from runoff routing are not considered as vegetation cover is sparse in the pilot study regions considered here (Section 2.3) and a simplified water balance approach is found to represent well the key hydrological fluxes in drylands [15]. Rather than estimating effective runoff and soil moisture through horizontal runoff routing, DryMOD aims to (i) assess the sensitivity of the rainfall partitioning into runoff and infiltration to spatially and temporally distributed rainfall inputs, and (ii) calculate vertical fluxes (runoff and soil moisture) according to spatially heterogeneous soil properties. This is useful in order to identify runoff-generating areas and characterize soil moisture patterns at the regional scale, and these key fluxes are temporally aggregated at the monthly time step. The objective here is to provide a model that is tightly integrated with the required data and which is based on few parameters so that it can make use of improved remote

sensing data with adequate spatial and temporal resolution and coverage. Thus, DryMOD can be used to gain insight into process dynamics across the spatio-temporal scales of the model, and to characterize regional-scale runoff and soil moisture over seasonal catchments as considered here.

2.3. Pilot Study Regions

Two hydrological catchments, in Tunisia and Senegal, are selected for the model evaluation undertaken here (Figure 2). The catchment boundaries are delineated from SRTM-3 (Shuttle Radar Topography Mission) Digital Elevation Model (DEM) data [16] using the catchment analysis function in the PCRaster GIS [12], and are used to define the model domain for DryMOD.

Figure 2. Hydrological catchment boundaries and elevation maps derived from the Shuttle Radar Topography Mission (SRTM) digital elevation model (DEM) for the pilot study regions in (**a**) Tunisia, and (**b**) Senegal.
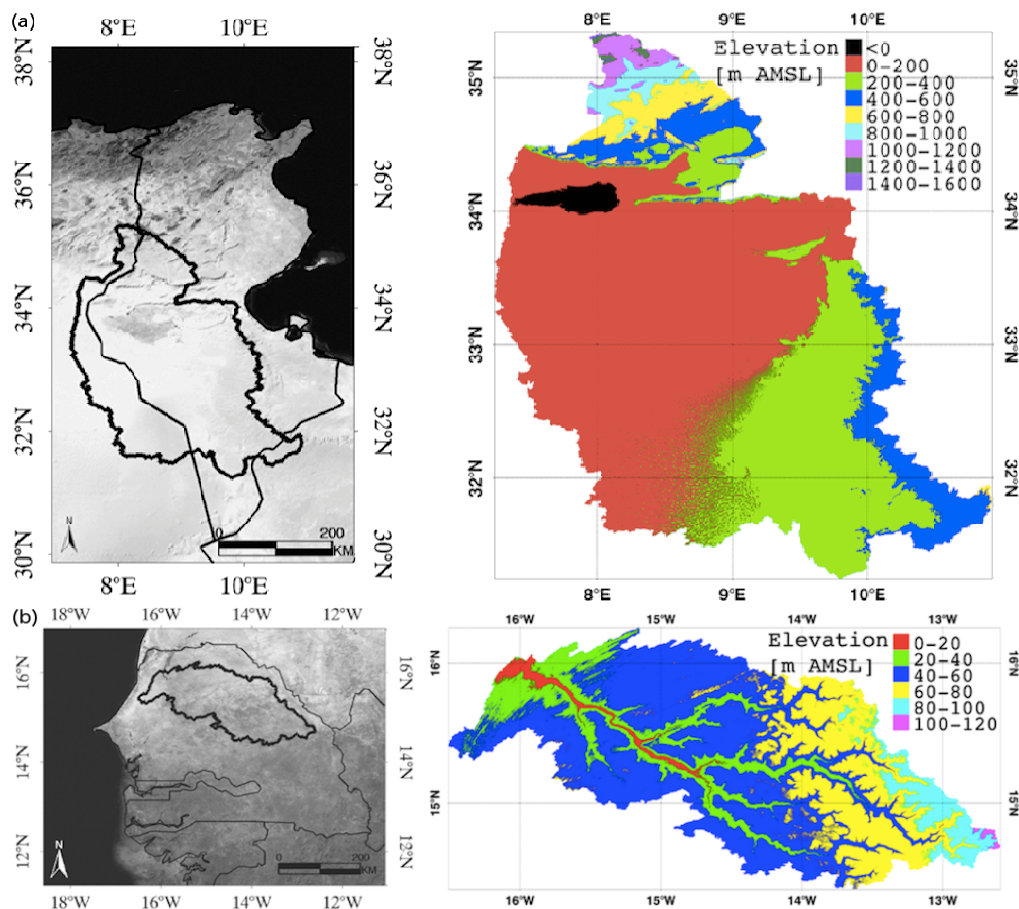

The catchment in Tunisia ($\sim$85,000 km^2) is a closed basin of an ephemeral salt lake, characterized by a strong N-S gradient of semi-arid to arid climate (400 to 70 mm annual rainfall) and predominantly winter precipitation. Rainfall intensity and frequency is important to this region as high-intensity rainfall of up to 360 mm·h^{-1} observed in the north can generate large volumes of surface runoff [17]. The main soil groups are regosols, which lie on soft rock, and lithosols, which lie on hard rock [18]. The catchment in Senegal ($\sim$43,280 km^2), an ephemeral stream in the Ferlo region, is part of the

Sahel bioclimatic zone. The area is characterized by arid to semi-arid climate with a cool dry season (November to June), hot humid summer (July to September), and annual rainfall between 200 and 500 mm (monthly maximum rainfall of 120 mm measured at the Linguère station) [19]. Soils in the region, especially brown and brown-red sub-arid soils, are not rich in minerals and are prone to degradation [20]. Both study sites are characterized by vegetation with sparse ground cover and relatively deep rooting systems (2.5–4.0 m), such as olive trees in Tunisia, and open shrubland species in Senegal that are well adapted to arid conditions.

3. Data and Methods

A flowchart of DryMOD, including the rainfall forcing, the inputs and parameterization data sources, as well as the processes represented and the relevant outputs is shown in Figure 3. This is followed by a description of the rainfall forcing, model stabilization and applications in the catchments considered here, and the methods for sensitivity analyses.

Figure 3. Flowchart of the DryMOD model: data inputs and outputs (parallelograms), parameters (rectangles), and decisions (diamond shape).
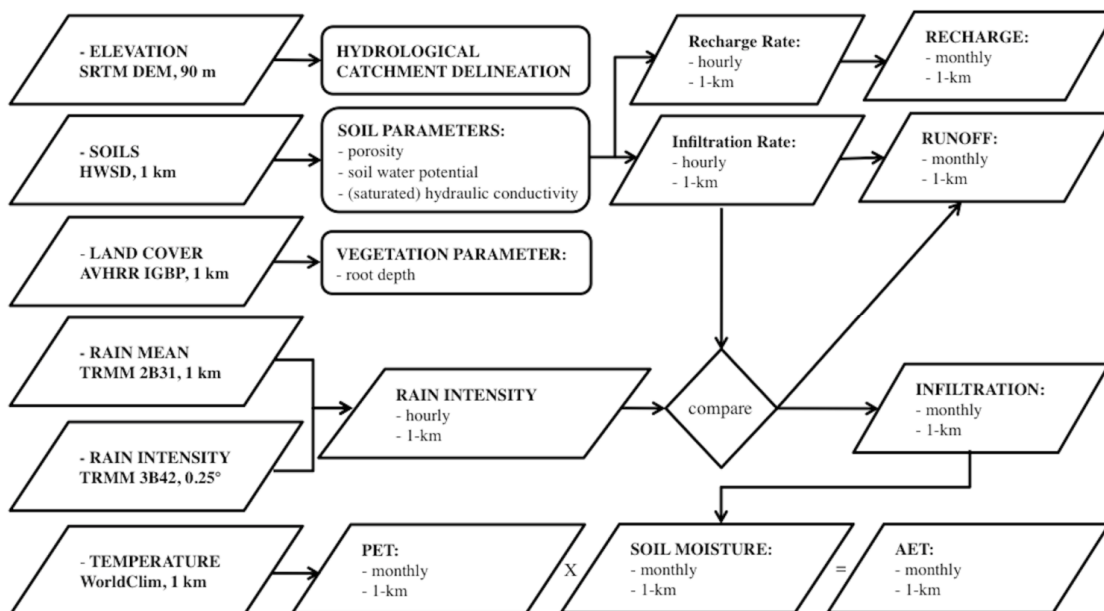
3.1. Rainfall Forcing

Distributed hydrological modeling requires information on rainfall intensities with temporal resolutions at scales smaller than monthly and daily means (ideally hourly or sub-hourly), as well as spatially continuous coverage and sufficiently high spatial resolution to capture the typical size of rainstorms (ideally 1–2 km spatial resolution). Rainfall data are increasingly provided at relatively high temporal resolution from remote-sensing based products. However, both high spatial and temporal resolutions are not provided by any one of the currently available global gridded rainfall datasets.

In order to combine the spatial and temporal detail from two different rainfall datasets, a novel method was developed for intensity correction and spatial disaggregation of TRMM 3B42 based

data [7,14] from 0.25° to 1-km resolution using a TRMM 2B31-based rainfall climatology [7,13]. The two datasets are derived from the standard NASA TRMM 2B31 and 3B42 V6 products [21,22]. The rainfall forcing dataset corrected for fractional cover of rainfall (FCR) and disaggregated to 1-km spatial resolution is referred to as FCR-corrected hereafter, while the dataset subjected only to disaggregation without intensity correction is termed non-corrected [7]. In the stochastic rainfall field generator (weather generator) of DryMOD, wet and dry hours are determined, based on the TRMM 2B31-based 1-km rainfall climatology. The gamma distribution function $\Gamma(x)$ parameters α and β (inferred from the 3-hour TRMM 3B42 based product [14]) are used to determine rainfall intensities at each hourly time step. Further details are provided in Section 1, Supplementary Material. This approach allows for simulation of rainfall with an hourly time step as relevant for dynamic partitioning of rainfall into infiltration and surface runoff, and for modification of soil moisture storage and infiltration rate. Monthly outputs of total simulated rainfall, runoff, infiltration, groundwater recharge, evapotranspiration, and resultant changes in soil moisture are automatically generated. Sections 4.1.2 to 4.1.4 describe the impact of this disaggregation and rainfall simulation on runoff and soil moisture dynamics and patterns.

3.2. Model Parameterization and Boundary Conditions

3.2.1. Soil Hydraulic Parameters

Soil water conditions and hydraulic conductivity are determined on the basis of soil information from the 1-km Harmonized World Soil Database (HWSD) [23] (see Section 2, Supplementary Material). Bulk density for the subsoil layer, which is used for calculating the recharge rate from the base of the soil profile, is derived according to the depth-dependency bulk density model for dryland soils in the Mediterranean [24] and Australia [25]. Bulk density increases with depth, while porosity decreases (hence, infiltration capacity into deeper layers of the soil profile decreases). The remaining soil parameters determining hydraulic properties are calculated using root depth to represent the soil profile in a spatially distributed manner on the basis that water reaching the profile below the rooting depth will generally be unavailable for transpiration and thus, available for recharge and deep percolation. Root depth is determined according to the 1-km spatial resolution AVHRR Global Land Cover (GLC) dataset [26] and the IGBP (International Geosphere-Biosphere Programme) vegetation codes (Table 2 in [27]) for the land cover types found in the two pilot study regions (see Section 2, Supplementary Material).

Based on the bulk density adjustment for root depth, an overall increase of bulk density by 0.2–0.6 g·cm^{-3} with increasing depth is observed for most soil profiles in the study regions. Since calculated bulk density values for the subsoil layer increase with depth, the porosity decreases. The decrease of porosity expressed with depth as volume fraction is between 0.1 and 0.4 for soil profiles in the two study regions. The general range of *b*-values (power of the soil moisture characteristic curve, see Section 2, Supplementary Material) is between 2.0 and 24.0 [28]. In both study regions *b*-values fall in the range of 2.0–8.0 with the exception of the clayey Solonchak soil profiles in the Tunisia study region where computed *b*-values are in the 12.0–14.0 range, that is approximately double those for other soil profiles. These soils are characterized by low bulk density, low sand content, and high clay

content and their porosity decreases by half from 0.4–0.5 to 0.2–0.3 with increasing depth, as calculated for topsoil and subsoil layers. Saturated hydraulic conductivity K_{sat} determines the ability of saturated soil to transmit water at a rate determined by hydraulic conductivity and depends mainly on pore size distribution but also on the properties of liquid water and vapor. In DryMOD, K_{sat} is derived in $kg \cdot s \cdot m^{-3}$ and converted to rate in $mm \cdot h^{-1}$ for the calculation of infiltration and recharge rates. The K_{sat} values for subsoil layers (not shown) decrease with increasing depth to values below $1.0\ mm \cdot h^{-1}$ for all soil profiles in the Tunisia ($K_{sat} = 0.1–1.0\ mm \cdot h^{-1}$) and Senegal ($K_{sat} = 0.2–0.7\ mm \cdot h^{-1}$) study regions.

3.2.2. Potential Evapotranspiration

The atmospheric moisture demand, potential evapotranspiration *PET* in mm, is estimated in DryMOD for months from January to December over each study region using mean monthly air temperature data from the WorldClim temperature climatology and the Thornthwaite model [29–32] including an adjustment for day length and solar angle [33] and heat index calculation (see Section 3, Supplementary Material). The WorldClim dataset provides a monthly air temperature climatology at approximately 1-km spatial resolution (30-arc seconds horizontal grid spacing) and covers the 1950–2000 time period [34]. As inter-annual changes of temperature are not considered in the DryMOD model, the January–December values (Section 3, Supplementary Material) are used to drive *PET* in the model for the stabilization and application runs over each study area.

3.2.3. Actual Evapotranspiration

Most ground weather stations provide meteorological data for calculation of PET, not AET. Various methods have been developed to derive AET as a function of PET and soil dryness [35,36]. In DryMOD, AET is derived from PET and soil dryness using the Budyko bucket model (Budyko and Zubenok, 1961 in [35–37]), according to which AET is specified as a function of PET in mm $month^{-1}$ and moisture availability θ as follows:

$$AET = PET \times f(\theta) \tag{2}$$

This general formulation allows for a reduction of evapotranspiration by available soil moisture where the $AET \sim f(\theta)$ relationship can be defined in different forms (Table 1, [36]). Equation (2) is implemented here due to its simplicity and because it was developed for the bucket-type soil moisture storage model implemented in DryMOD.

3.2.4. Soil Moisture

In DryMOD, soil moisture θ expressed as volumetric fraction (m^3 water $\cdot$ m^{-3} soil) is calculated every monthly time step *t* according to the following equation:

$$\theta_t = \theta_{t-1} + (I_t - AET_t - GWR_t) \tag{3}$$

where θ_{t-1} is soil moisture at the previous time step plus net soil moisture change for the current time step *t*, calculated as infiltration *I* less actual evapotranspiration *AET* and groundwater recharge *GWR*; all units are converted to fractional water content through division by the root depth. The change in

soil moisture $\Delta\theta$ is the amount of water added or removed from the initial soil moisture level and the values range between zero and field capacity minus wilting point. Specifically, in DryMOD, soil moisture is calculated according to a bucket type model where soil moisture content θ is limited at the lower and upper bounds, respectively, by soil moisture at wilting point θ_{WP} (dry soil) and soil moisture at field capacity θ_{FC} (wet soil) as follows:

$$
\begin{array}{ll}
\theta - \theta_{FC} & if \quad \theta \geq \theta_{FC} \\
\dfrac{\theta - \theta_{WP}}{\theta_{FC} - \theta_{WP}} & if \quad \theta_{WP} < \theta < \theta_{FC} \\
0 & if \quad \theta \leq \theta_{WP}
\end{array}
\tag{4}
$$

For the stabilization run θ is initialized as θ_{FC}, *i.e.*, assuming nearly saturated conditions (because θ can be different than θ_{FC} and is usually smaller than porosity due to entrapped air in the soil), and rapidly reaches a dynamic equilibrium. Initial infiltration and recharge rates expressed in mm·h^{-1} are calculated using hydraulic conductivity equations (detailed in Supplementary Material, Section 2) with the parameters for topsoil and subsoil as indicators of hydraulic properties at the soil surface and at the base of the soil profile, respectively. At the monthly time step of the model, soil moisture is calculated according to Equation (3), taking into account antecedent moisture conditions from the previous month, and the net change of soil water content, *i.e.*, infiltration less AET and GWR. Thus, soil moisture calculated in DryMOD describes the quantity of moisture gains and losses, as well as the frequency of hydrological deficits as these have critical implications for optimization of agricultural activities.

Table 1. Soil parameter values and summary statistics for the randomly selected 1-km pixel in (**a**) Tunisia, and (**b**) Senegal considered in the sensitivity analysis.

Parameter (Units)	Nominal Value	−50% of Nominal Value	+50% of Nominal Value	Min	Max	Mean	Std. Dev.
(a) Tunisia							
X1: porosity topsoil (-)	0.47	0.24	0.71	0.36	0.54	0.43	0.05
X2: porosity subsoil (-)	0.28	0.14	0.43	0.12	0.34	0.20	0.08
X3: ksat_topsoil (kg·s·m^{-3})	7.08	3.54	10.63	2.01	13.51	4.84	3.33
X4: ksat_subsoil (kg·s·m^{-3})	4.10	2.05	6.16	1.57	6.15	2.86	1.20
X5: *b*-value (-)	0.25	0.12	0.37	0.00	0.98	0.52	0.34
X6: root_depth (m)	2.50	1.25	3.75	1.50	6.00	3.89	0.33
(b) Senegal							
X1: porosity topsoil (-)	0.48	0.24	0.71	0.35	0.48	0.39	0.06
X2: porosity subsoil (-)	0.32	0.16	0.48	0.13	0.99	0.19	0.08
X3: ksat_topsoil (kg·s·m^{-3})	7.22	3.61	10.83	2.35	7.22	3.93	2.24
X4: ksat_subsoil (kg·s·m^{-3})	3.14	1.57	4.71	1.46	4.10	2.15	0.89
X5: *b*-value (-)	0.26	0.13	0.39	0.22	0.67	0.51	0.18
X6: root_depth (m)	2.50	1.25	3.75	1.50	4.00	3.05	0.48

3.2.5. Infiltration and Groundwater Recharge

DryMOD uses the hydraulic conductivity of the soil to calculate hourly infiltration and recharge rates, along with a water mass balance approach to calculate recharge [28]. Monthly cumulative

Infiltration *I* for a given grid cell is the sum of hourly-based infiltration for wet hours during that month if the soil profile is not saturated; at saturation (*i.e.*, when accumulated soil moisture exceeds soil moisture at field capacity), water infiltrated through the soil profile percolates to groundwater recharge. The hydraulic conductivity of subsoil layers determines the rate of recharge in bucket-type soil water models (for details, see [25,38] and Supplementary Material, Section 2). The water percolating to the bottom layer of the soil is cumulated as groundwater recharge *GWR* expressed as mm month^{-1} and used in the soil water balance model (Equation (3)). Thus, in DryMOD cumulative infiltration and groundwater recharge are recorded as model outputs for each monthly time step.

3.2.6. Runoff

Surface water runoff is a major and important source of freshwater in dryland regions characterized by low rainfall amounts, high spatial and temporal variability of rainfall, and high salinity of groundwater sources [39]. Runoff in drylands is commonly collected through traditional water harvesting techniques and presents an important contribution to available water mainly for agricultural uses such as dryland farming and livestock. Thus, knowledge of runoff generation areas is essential for the effective planning of water harvesting systems in drylands, as well as for optimization of agricultural activities. Hence, the aim here is to estimate the fraction of rainfall that becomes runoff (runoff ratio) and to identify areas in the pilot study regions that are likely to generate runoff.

Measurements of runoff are generally unavailable in dryland regions mainly due to the costs and logistics involved in maintaining stream gauges in rivers with infrequent but sediment-laden storm flow [40], as well as in ephemeral streams in dryland countries [10,11]. Instead, runoff is estimated through water balance models, in which rainfall arriving at the soil surface is partitioned into infiltration and runoff according to soil hydraulic properties. In DryMOD, this is achieved by allowing for occurrence of both infiltration excess and saturation excess runoff. Within a given monthly time step, the runoff process is driven by the hourly rainfall simulation model, in which rainfall is partitioned into infiltration and changes in groundwater recharge and soil moisture according to a saturation excess model [41] (Section 2, Supplementary Material).

For non-saturated profiles, infiltration occurs (at the infiltration rate) until soil moisture reaches field capacity, *i.e.*, the profile is nearly saturated. The hourly infiltration rate is updated according to the exponential model illustrated in Figure S1 (Supplementary Material, Section 2). For saturated soil profiles, groundwater recharge occurs (at the groundwater recharge rate) and any excess water is cumulated. The bucket-type model allows for recharge under soil moisture at saturation because features such as fractured soils and salt depressions with moist surface due to shallow water table are common to interior drainage basins in drylands [42]. At the end of the monthly time step, runoff is the excess rainfall at the surface that did not evaporate or infiltrate into the soil profile. From month to month, soil moisture is updated according to Equation (3), which accounts for antecedent moisture conditions, infiltration, actual evapotranspiration, and groundwater recharge.

3.3. DryMOD: Model Stabilization, Applications, and Sensitivity Analysis

3.3.1. Model Initialization and Stabilization

DryMOD is initialized with a stabilization (spin-up) run over 10 years driven by seasonally and inter-annually varying rainfall and seasonally varying temperature. In the spin-up run, initial soil moisture is set at θ_{FC}, and initial infiltration and groundwater recharge rates are calculated according to the method based on hydraulic conductivity, soil depth, and porosity of the topsoil and subsoil layers, respectively. The aim of the model spin-up run is to (a) provide realistic estimates of initial soil moisture conditions for the model applications over each pilot study region considered here; and (b) assess the effect of using the non-corrected and FCR-corrected rainfall forcing data on soil moisture stabilization. The spin-up run ensures that the model parameters are at equilibrium with initial conditions at the start of the model applications and avoids errors associated with model equilibration.

A trend toward stabilization of soil moisture from initial values of 0.215 m^3·water·m^{-3} soil for Tunisia and 0.19 m^3·water·m^{-3} soil for Senegal is apparent in the first two years of the model spin-up run (*i.e.*, time steps 1–24 of 120) for both study sites and both the non-corrected and FCR-corrected rainfall forcing datasets (results not shown). However, soil moisture derived with the non-corrected rainfall stabilizes at lower values than soil moisture derived with the FCR-corrected rainfall forcing. Specifically, soil moisture stabilizes around 0.11–0.12 and 0.12–0.13 m^3·water·m^{-3} soil for Tunisia, and between 0.11–0.13 and 0.11–0.14 m^3·water·m^{-3} soil for Senegal with the non-corrected and FCR-corrected rainfall data forcing, respectively.

3.3.2. Model Applications to Pilot Study Regions

The model applications for the two study sites in Tunisia and Senegal use the soil moisture distribution maps produced by the stabilization runs with the non-corrected and FCR-corrected rainfall datasets, respectively, as initial maps of soil moisture conditions and run over 10 years for each simulation. This is to test the sensitivity of the key hydrological components, surface water and soil moisture, to changes in the representation of input variables with a specific focus on the use of non-corrected and FCR-corrected rainfall data. If the model is found to be sensitive to the rainfall data inputs, the expectation is that using the FCR-corrected TRMM based data will produce rainfall that generates runoff as compared to non-corrected data, which underestimates rainfall intensities and thus, is not expected to result in realistic runoff [7]. If the model is found to be insensitive to the different rainfall inputs, this would mean that the runoff generation is either uniformly distributed within the study region regardless of the spatial characteristics of simulated rainfall time-series, or the rainfall simulation technique fails to represent the characteristic spatial distribution of rainfall at the 1-km spatial scale. The expectation is that the rainfall simulated with the FCR-corrected data will realistically represent the rainfall properties as observed in the 1-km TRMM 2B31-based rainfall climatology and will result in simulation of higher runoff due to accounting for the sub-grid spatial variability of rainfall [7]. Model applications in the two pilot study regions in Tunisia and Senegal allow for an assessment of the hydrological significance of simulating rainfall with spatial and temporal disaggregation. Results from the model applications with rainfall simulations based on

the non-corrected and FCR-corrected TRMM based data are presented and evaluated through sensitivity analysis.

3.4. Sensitivity Analysis

The objective here is to examine the sensitivity of rainfall simulation (Section 4.1.1) and runoff-generating areas and soil moisture distribution (Section 4.1.2) to data inputs from the non-corrected and FCR-corrected rainfall datasets. This also includes analysis of runoff and soil moisture dynamics over selected ground weather stations (Section 4.1.3) and characterization of runoff generating rainfall intensities (Section 4.1.4). The second part of the sensitivity analysis (Section 4.2) evaluates the sensitivity of runoff and soil moisture simulations with the non-corrected and FCR-corrected rainfall intensities to varying hydraulic properties over each study region. For this purpose, soil parameters are varied one at a time, while the changes in the output (simulated monthly runoff and soil moisture) are monitored. Specifically, six input soil parameters, to which runoff and soil moisture are expected to be sensitive (Table I in [43])—topsoil and subsoil porosity, topsoil and subsoil saturated hydraulic conductivity, the *b*-value, and root depth—are varied over 12 months for a randomly selected location in each pilot study region. The base run uses the nominal values of all soil hydraulic parameters for the selected location, while in each sensitivity analysis run one of the soil parameters is varied from −50% to +50% of its nominal value at that location with a 10% step change, while the other soil parameters remain fixed. The results are reported as percentage change *PC* in the output variable *Y* according to the following equation:

$$PC_{Y(x)} = \left(\frac{Y(x) - Y_{base}}{Y_{base}} \right) \times 100 \tag{5}$$

where $Y(x)$ is simulated runoff or soil moisture when varying the input soil parameter x and Y_{base} is simulated runoff or soil moisture in the base run. Additionally, the first order sensitivity index FOSI [44] is calculated based on the variance *Var* of $Y(x)$ and Y_{base} according to the following equation:

$$FOSI_{Y(x)} = \frac{Var(Y(x))}{Var(Y_{base})} \tag{6}$$

While the *PC* measure can be used to assess the magnitude of changes in the output variable driven by individual input soil parameters, the *FOSI* variance-based measure can be used as a guide in prioritizing subsequent model calibration and optimization tasks [44]. The *FOSI* measure also provides information on the relative importance of individual soil parameters in driving changes in the output variables runoff and soil moisture.

4. Results and Discussion

4.1. Model Applications to the Pilot Study Regions

The soil moisture fields derived in the model stabilization run with non-corrected and FCR-corrected TRMM based data are used for model initialization here, over 10 years, for each pilot region. In the absence of detailed information for validation, estimates of runoff and soil moisture

generated with the DryMOD model using the non-corrected and FCR-corrected rainfall datasets are compared with values reported in the literature for similar dryland environments. Additionally, runoff and soil moisture dynamics are examined for a selected location in each pilot study region. This section concludes with analyses of hourly-based rainfall-runoff dynamics allowing for characterization of runoff-generating rainfall intensities.

Figure 4. Density plots of mean monthly rainfall simulated over 10 years with the non-corrected and corrected for fractional cover of rainfall (FCR) TRMM 3B42 based rainfall data against TRMM 2B31 based mean monthly rainfall climatology across the catchments in (**a**,**b**) Tunisia and (**c**,**d**) Senegal. Red indicates high, white indicates low 1-km pixel densities.
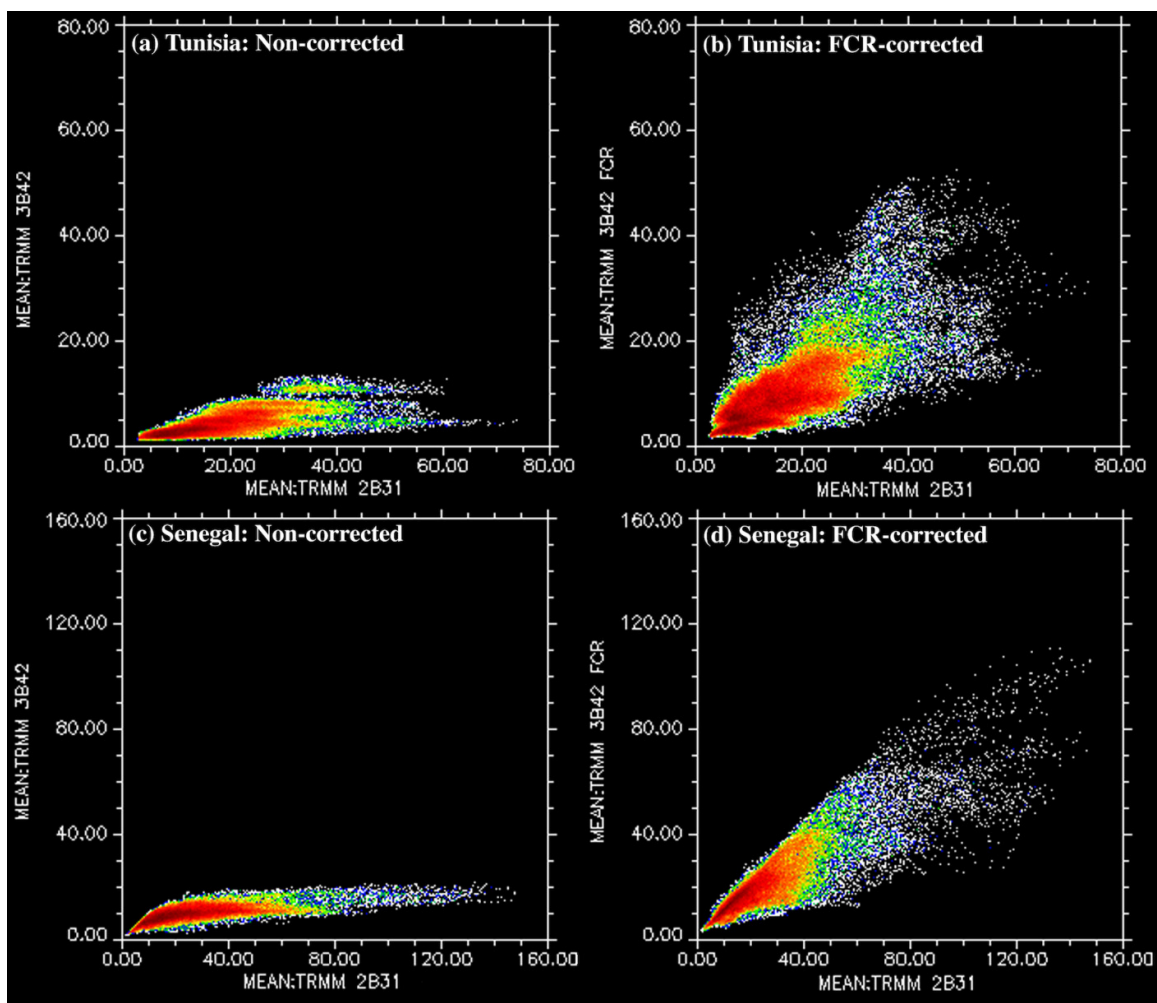
4.1.1. Sensitivity of Rainfall Simulations to TRMM-Based Input Datasets

The evaluation of the algorithm for spatial disaggregation and intensity correction of the TRMM based rainfall time-series [7] encouraged further investigation of its contribution to water balance modeling in drylands. As there is little ground-based data for direct comparison against spatial rainfall fields of hourly rainfall intensity, the contribution of improving the rainfall representation in the model

is assessed through sensitivity analysis of monthly rainfall fields simulated with the non-corrected and FCR-corrected rainfall forcing, respectively. Simulated monthly rainfall fields generated with the non-corrected and the FCR-corrected data are averaged over 10 years for comparison with the original TRMM 2B31-based rainfall climatology (Figure 4). This helps to identify if the non-corrected or the FCR-corrected TRMM-based rainfall intensities provide a more realistic representation of rainfall according to the 1-km TRMM 2B31-based rainfall climatology.

As expected, the simulated intensities are unrealistically small for the non-corrected TRMM-based rainfall data (Figure 4). Given the generally low probability of rainfall, when the non-corrected rainfall data are used the maximum number of possible rain hours is exceeded before the mean monthly rainfall for a given 1-km pixel is reached according to the TRMM 2B31 based climatology ±20% variance. This results in substantially lower mean monthly rainfall estimated with the non-corrected (Figure 4a,c) as compared to the FCR-corrected rainfall data (Figure 4b,d). While the annual average of mean monthly rainfall ranged between 0 and 80 mm for Tunisia and between 0 and 160 for Senegal in the TRMM 2B31-based data, the use of the non-corrected dataset failed to generate sufficient rainfall for all 1-km pixels in both study regions (Figure 4a,c). The FCR-corrected dataset resulted in mean monthly totals that more closely represent those derived from the TRMM 2B31 based rainfall climatology across both study regions (Figure 4b,d). This confirms that it is not realistic to assume even distribution of non-corrected TRMM-based rainfall intensities at the sub-0.25° grid-cell scale as these values represent an average over large area covered by a given 0.25° grid cell and fail to capture localized convective storms. Thus, FCR-correction of TRMM 3B42-based rainfall intensities is a recommended step of the disaggregation to 1-km for detailed analysis of rainfall intensities, such as in hydrological model forcing.

4.1.2. Sensitivity of Runoff and Soil Moisture to Rainfall Forcing with TRMM-Based Input Datasets

Runoff Generating Areas

As non-corrected TRMM based rainfall data underestimate rainfall intensities and monthly totals, when used in a stochastic weather generation algorithm these will produce unrealistically low runoff. Thus, the expectation is that rainfall simulations based on the FCR-corrected dataset will generate more runoff in parts of the pilot study regions during high-intensity rainfall events.

As shown in Figure 5, for both study regions, the mean monthly runoff generated with the non-corrected dataset is very small, partly due to no runoff generated for most summer months, which are dominated by convective rainfall. The results here are in agreement with those reported in previous work on the spatial and temporal resolutions required for realistic hydrological modeling in drylands. As demonstrated in several studies [9–11], spatial averages of rainfall intensities over areas larger than 2 km^2 fail to generate runoff due to their inability to capture the space-time variability of convective rainfall, which operates at hourly and sub-hourly temporal scales and spatial scales of 1–2 km^2. Moreover, previous work in similar dryland regions showed that the highest rainfall intensities are sustained over small space-time scales [10,11,45]. For example, the spatial variability of rainfall over small distances in the Sahel can be approximately 20 mm over a 3 km distance [46]. Indeed this characteristic spatio-temporal variability of rainfall provided the motivation for the spatial disaggregation

and intensity correction of the TRMM 3B42-based time-series introduced here. The evaluation presented here confirms the relevance of the FCR correction, which allows for dynamic simulation of rainfall making best use of TRMM 3B42 and TRMM 2B31-based datasets, and highlights the sensitivity of runoff to rainfall forcing.

Figure 5. Mean monthly runoff calculated as a 10-year average from the regular model runs with the non-corrected and FCR-corrected TRMM-based rainfall forcing for the pilot study regions in (**a,b**) Tunisia and (**c,d**) Senegal.
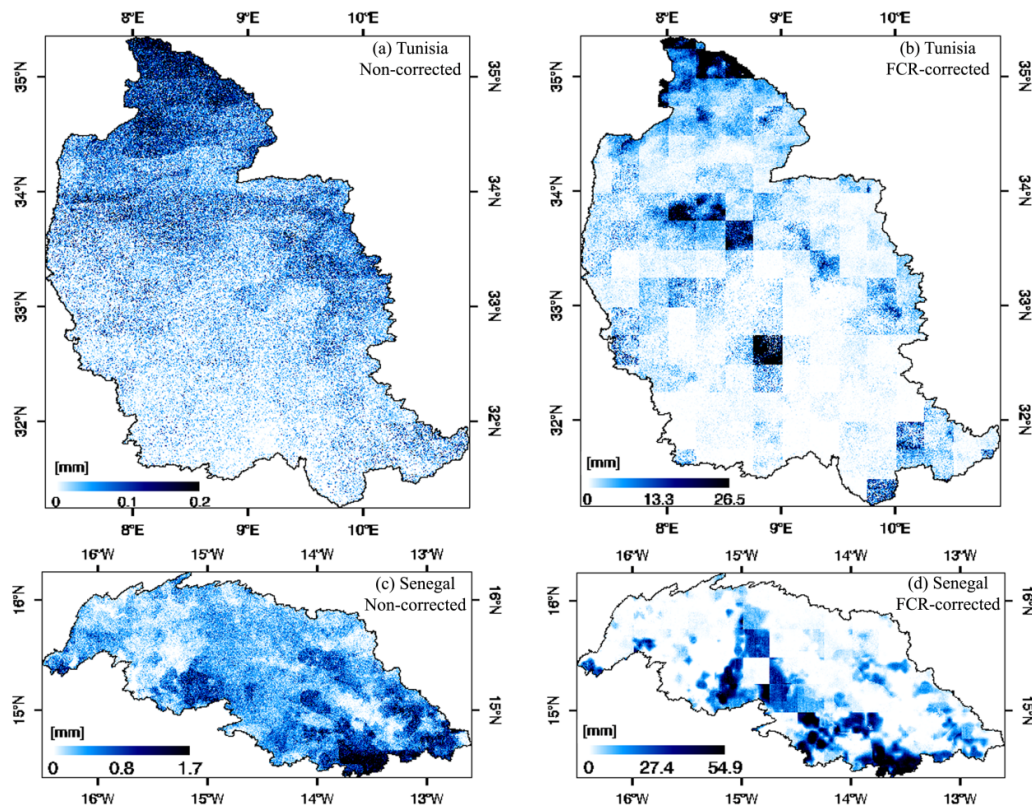
On average, approximately 50% more runoff is generated in the Senegal than in the Tunisia catchment as estimated from the 10-year long regular run of the model, reflecting the fact that runoff is dominated by higher rainfall in Senegal as compared to Tunisia (Figure 5). While runoff harvesting is widespread in Tunisia, the results presented here suggest that the Senegal study region can also benefit substantially from water harvesting schemes, especially during the rainy summer months between June and September. Although the Senegal study region is relatively flat, rainwater harvesting and encouragement of re-infiltration of overland flow can take many forms (e.g., small water-retention dams, small dykes or gradients) and can enhance water supply in months of water scarcity as demonstrated for crop cultivation, especially in the western and southern part of the region [46]. For the study region in Tunisia, the results indicate that agriculture can benefit from water harvesting schemes throughout nearly the entire year, albeit with relatively lower volumes of runoff than in Senegal as estimated here.

In summary, the application of the model for the two pilot study regions confirms the contribution of FCR-corrected TRMM-based data for simulation of important hydrological fluxes such as runoff.

Indeed the runoff component was shown to be sensitive to the different input rainfall datasets and the use of the FCR-corrected rainfall dataset is recommended unless a full model validation for a gauged catchment can be carried out.

Soil Moisture Distribution

The focus here is on the spatial distribution of soil moisture estimated in the regular model runs over Tunisia and Senegal using the FCR-corrected rainfall data, as soils play a key role in storing water so that it is available for vegetation growth. The seasonal distribution of soil moisture is represented for each month as a 10-year average, derived from the regular runs of DryMOD using the FCR-corrected rainfall data for Tunisia and Senegal (Figure 6).

Figure 6. Mean monthly soil moisture calculated as a 10-year average from the regular model runs with the FCR-corrected TRMM-based rainfall forcing for (**a**) Tunisia and (**b**) Senegal.

(**a**) (**b**)
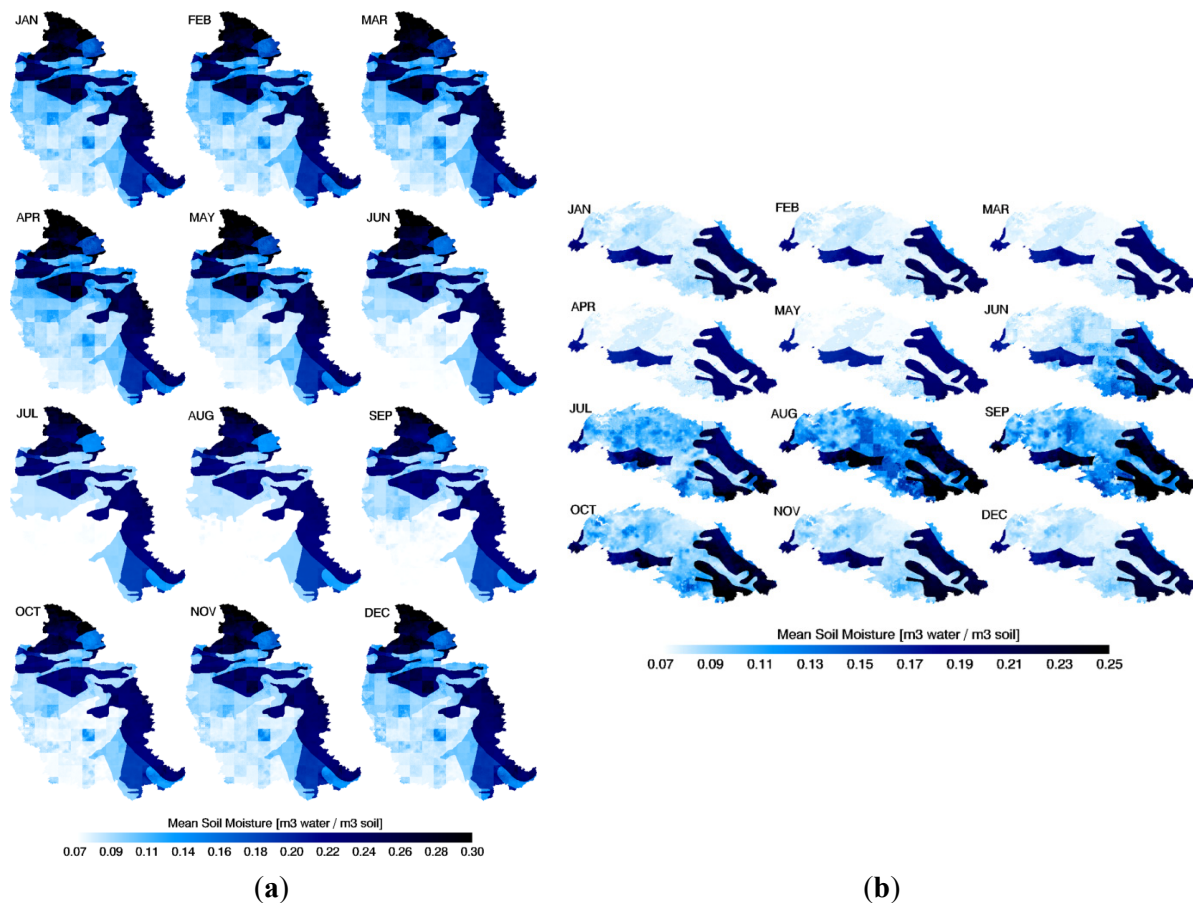
The temporal variability of soil moisture is directly related to the variability of water inputs through rainfall with peaks of soil moisture during and shortly following rainy months for each study region. Where soil moisture is lowest, the artifacts related to the 0.25° TRMM grid cells observed in the runoff maps are also present in the soil moisture maps for both study regions. Mean soil moisture fractional content ranged between 0.07 and 0.30 $m^3 \cdot water \cdot m^{-3}$ soil in the Tunisia study region and between 0.07 and 0.25 $m^3 \cdot water \cdot m^{-3}$ soil in the Senegal study region. This is at least partially explained through the higher runoff generated over the Senegal study region than that over the Tunisia catchment, the type of

vegetation cover (shallower rooting depths in the Senegal region), and the water holding capacities of soils in the Senegal as compared to the more arid Tunisia study region. It is worth noting that soil moisture in the northern part of the Tunisian catchment is higher than in the south, due to higher rainfall, more pronounced topography (thus, lower temperatures) and differences in vegetation cover, affecting rooting and, thus, soil depth.

Unlike runoff maps, the soil moisture maps more clearly express the effects of soil mapping units, for which soil data was used for model initialization, especially that of calculated saturated hydraulic conductivity K_{sat}. Soils with higher K_{sat} values remained relatively wet throughout the year. The effects of temperature and root depth through evapotranspiration are also reflected in the spatial distribution of soil moisture. In both study regions higher soil moisture values are observed for areas of higher rainfall and lower temperatures with more expressed seasonal patterns of wetting and drying for soils with lower K_{sat} and higher root depths.

4.1.3. Runoff and Soil Moisture Dynamics over Selected Ground Weather Stations

Further examination of runoff and soil moisture changes for locations selected over a ground weather station in each study region shows clear seasonal response of these to rainfall forcing based on the non-corrected and FCR-corrected TRMM-based datasets, as well as to soil properties and root depth. The pixel selected in the Tunisia study region over the Tozeur station represents loamy-sand soils with root depth of 4.0 m characteristic to vegetation types with sparse ground cover and deep root systems that are well adapted to arid conditions. The pixel in the Senegal study region over the Linguère station represents a sandy soil with root depth of 3.1 m corresponding to the open shrubland cover type. Figure 7 shows the evolution of runoff and soil moisture in response to different rainfall input datasets over the monthly time steps of the 10-year model runs.

Water storage capacities (difference between volumetric soil moisture content at field capacity and that for dry soils) are generally between 3% and 6% for sand and 15%–25% for clay [47]. Similar water storage capacity values were reported for experimental plots in semi-arid Spain for loamy sand (5.2%–10%), sand (around 6.1%), and sandy loam (6.3%–7.1%) soils [48]. Increasing water storage capacity from 6.2% to 11.5% to 17.6% for decreasing sand fraction content from 94% to 65% and 23%, respectively, were reported for semi arid soil conditions [49]. For the locations selected here, soil moisture values expressed as percent are higher than reported figures, *i.e.*, between 20% and 28% for the pixel with loamy sand soils in Tunisia and between 20% and 40% for the pixel with sand soils in Senegal. While the reported figures are from plot-scale field experiments, the estimates here are dependent on the soil databases and root depth information used for model parameterization.

As with the results for runoff averaged across each catchment, the non-corrected TRMM based rainfall forcing fails to produce runoff in the selected locations or produces very low runoff (Figure 7a,c). Runoff in both locations occurs in months of relatively high water input through rainfall (*i.e.*, April–May and September–October in Tunisia and August–September in Senegal) with no runoff during most other time steps of the model runs. Runoff generation also depends on soil texture and physical properties with lower runoff from soils with high sand content than from those with high clay content [47]. However, for the locations selected more runoff was generated for the pixel with sand soils (90% sand) in Senegal than for that with loamy sand soils (86% sand) in Tunisia. This highlights

the importance of rainfall intensities for runoff generation, and the focus of the next section is on characterization of runoff generating rainfall intensities.

Figure 7. Sensitivity of runoff and soil moisture to the non-corrected and FCR-corrected TRMM based rainfall forcing for the location of the Tozeur ground weather station in Tunisia (**a**,**b**) and the Linguère ground weather station in Senegal (**c**,**d**) over the 10-year regular model runs (*i.e.*, 120 monthly time steps).
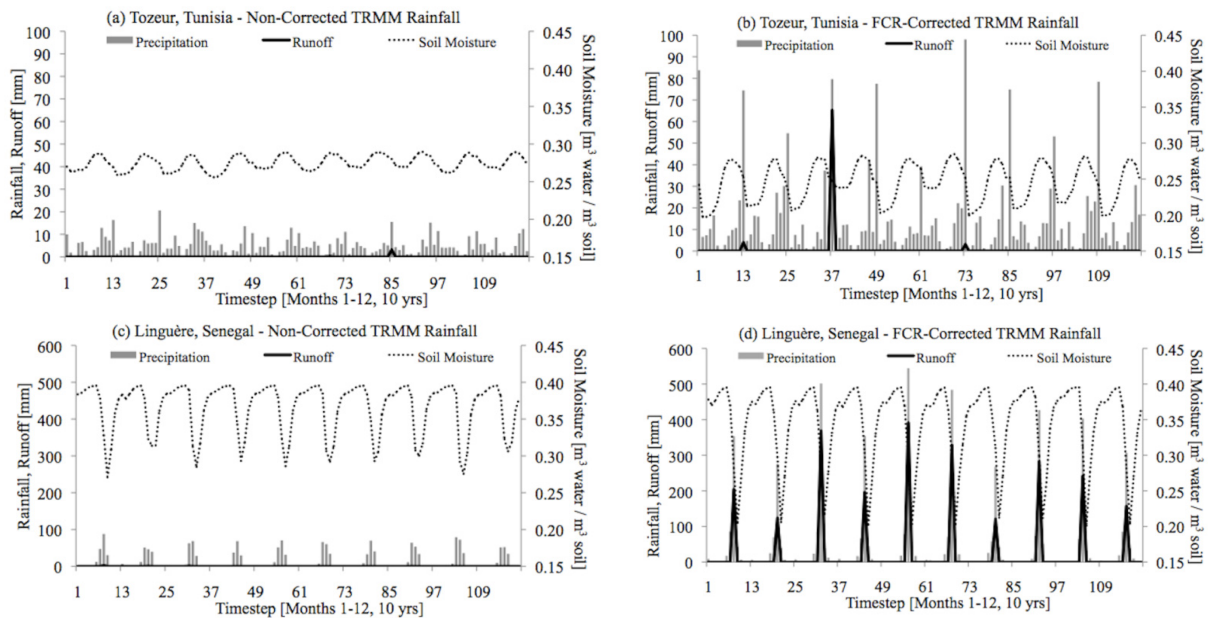
### 4.1.4. Runoff Generating Rainfall Intensities

An investigation of hourly dynamics of rainfall and runoff generation helps to identify the rainfall intensities that generate runoff in each of the catchments. Hourly rainfall intensities for each location are summarized into frequency distributions for the non-corrected and FCR-corrected TRMM-based rainfall datasets. For both study regions, substantially higher rainfall intensities are observed when the FCR-corrected rainfall datasets are used in the regular run of the DryMOD model (Figure 8).

For the Tozeur station in Tunisia most frequent are rainfall intensities of approximately 4–8 mm·h^{-1}, while for the Linguère station in Senegal, most frequent are intensities around 5–20 mm·h^{-1} (Figure 8). However, the non-corrected rainfall dataset fails to produce rainfall intensities higher than 7.19 mm·h^{-1} for the location in Tunisia and 5 mm·h^{-1} for the location in Senegal, while the FCR-corrected dataset produced rainfall intensities of up to 230 mm·h^{-1} for Tozeur and 40 mm·h^{-1} for Senegal. Although rainfall intensity data are not available for the selected stations, previous work indicates that 50% of rainfall in similar regions reaches the surface with intensities ≥ 27 mm·h^{-1} [46] and ≥ 32 mm·h^{-1} [50]. Thus, the FCR-corrected rainfall intensities appear more realistic.

Runoff-initiating rainfall rates depend on soil properties (soil type, texture, chemical properties) and in similar dryland environments range between 4.5 and 11 mm·h^{-1} with final infiltration rates of 5–50 mm·h^{-1} [39]. As illustrated in Figure 8, 95% of rainfall intensities ≥ 14.38 mm·h^{-1} generated runoff in the selected 1-km pixel for the Tunisia catchment. Similarly, Figure 8 shows that 96% of

rainfall intensities ≥ 5 mm·h^{-1} generated runoff for the selected 1-km pixel in the Senegal catchment. Although model-based estimates are difficult to validate against field-based measurements, and such measurements are not available here, the estimates here agree with reported observations of the non-linear response of runoff generation in arid regions (Brown and Wheater, 1989 in [10,39]). It is worth noting that while in the selected location in Tunisia the runoff generating rates are spread across a range of rainfall intensities, in the selected location in Senegal most of the runoff is generated by lower-intensity but more frequent rainfall events.

Figure 8. Frequency distributions of hourly rainfall and infiltration rates, and runoff derived from the 10-year model runs with non-corrected and corrected for fractional cover of rainfall (FCR) TRMM-based datasets for a 1-km pixel over (**a**,**b**) the Tozeur station in Tunisia and (**c**,**d**) the Linguère station in Senegal.
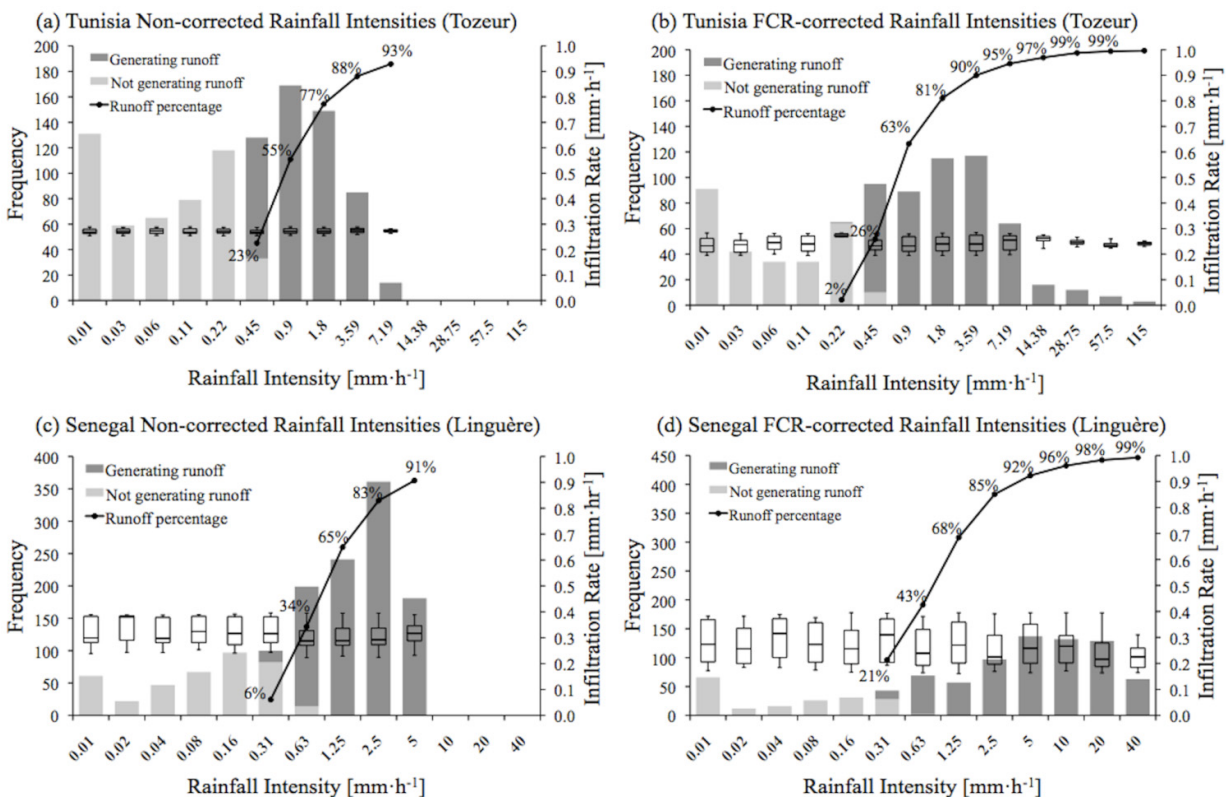

The analysis of hourly-based dynamics of runoff generation confirms the effectiveness of the intensity correction and spatial disaggregation of the TRMM 3B42-based data and suggests that the DryMOD model is robust for the regional applications in Tunisia and Senegal under differing hydro-climatic characteristics.

4.2. Sensitivity Analysis of Runoff and Soil Moisture to Soil Hydraulic Parameters

The sensitivity of the main hydrological fluxes (runoff and soil moisture) to six key soil hydraulic parameters that control the processes of infiltration, runoff, groundwater recharge, and evapotranspiration are examined here. A modified version of DryMOD for sensitivity analysis is

initialized here with the soil moisture conditions derived from the stabilization run of the DryMOD model using the FCR-corrected rainfall forcing for a randomly selected location in each study region. This represents the base run, against which subsequent sensitivity analysis runs are compared. In each of the six sensitivity analysis runs of the DryMOD model for the selected location, one of the six parameters was varied in a range from −50% to +50% of its nominal value with a 10% increment, while the other five remained fixed at their nominal value (Table 1). The base run and all subsequent runs are carried out over one year for each pilot study region. The sensitivity analysis plots are presented in Figure 9 for Tunisia and in Figure 10 for Senegal.

Figure 9. (**a**,**b**) Percent change and (**c**,**d**) first order sensitivity index (FOSI) for runoff (**left**) and soil moisture (**right**) for Tunisia.
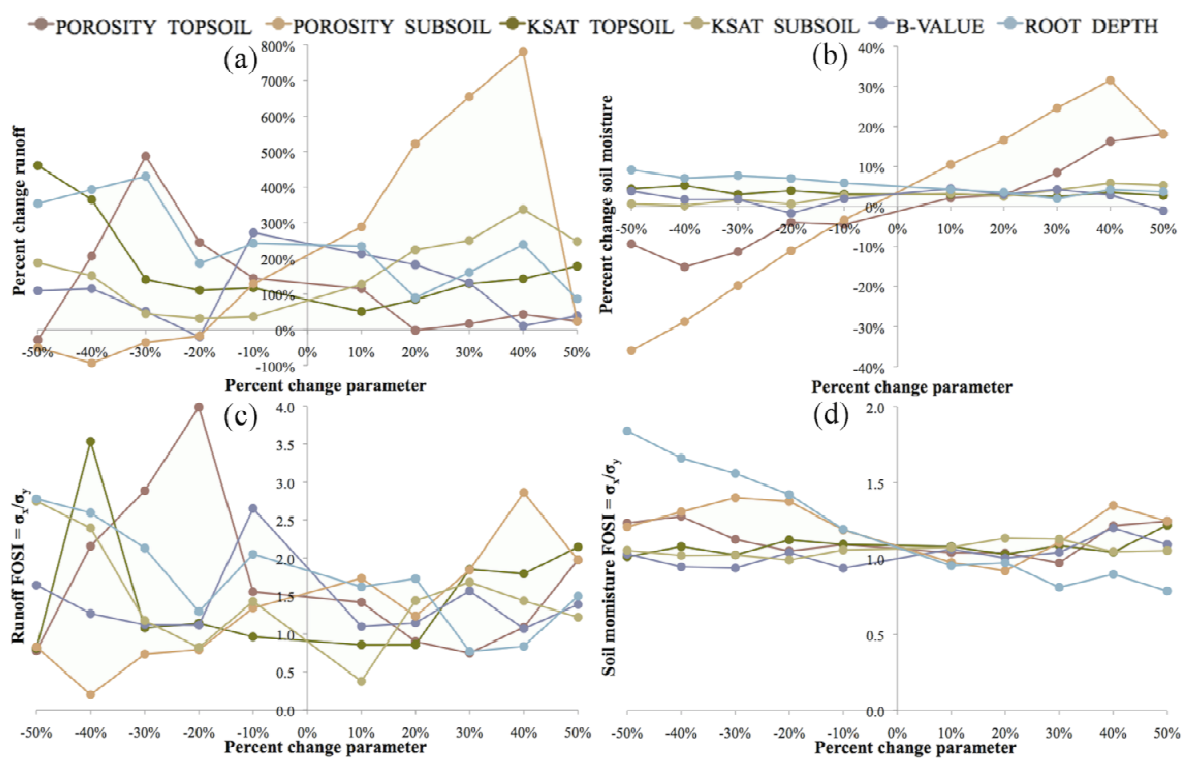

The plots of percent change for both study regions show that runoff (Figures 9 and 10, left) is more sensitive than soil moisture (Figures 9 and 10, right) to most of the parameters considered. With respect to runoff, both sensitivity metrics, *PC* and *FOSI*, are generally higher for Tunisia than for Senegal, while for soil moisture there are no substantial differences between the two pilot study regions. According to the *PC* metric with values above 100% for Tunisia (Figure 9, top) and above 30% for Senegal (Figure 10, top), runoff calculations are sensitive to the majority of parameters considered. With respect to the *PC* metric, soil moisture calculations show the largest sensitivities to porosity of the topsoil and subsoil for both study sites. The *FOSI* plot for Tunisia (Figure 9, bottom) shows that most variance in runoff is caused by changes in porosity and K_{sat} of topsoil. For Senegal (Figure 10, top), the most variance in runoff is induced by saturated hydraulic conductivity of topsoil. The *FOSI* plots of soil moisture for both study regions show that most of the variance is due to the

decrease of root depth and changes in the porosity of the topsoil and subsoil (Figures 9 and 10, bottom right).

The greatest changes in runoff and soil moisture are in response to changes in porosity of the topsoil and subsoil with the latter affecting drainage from the bottom of the soil profile and thus, infiltration capacity. As the porosities of the topsoil and subsoil increase, soil moisture increases due to increased infiltration capacity; as topsoil porosity decreases, runoff increases due to reduced infiltration capacity of the soil surface layer. Additionally, as root depth decreases, runoff increases as the soil profile is shallower and saturates more rapidly. For both study sites, greatest variances in runoff were observed when the input parameters decreased with the exception of Senegal where topsoil and subsoil porosity increase resulted in substantial variances in soil moisture calculations (Figure 10, bottom right). Most expressed were the impacts of a decreasing topsoil porosity and K_{sat} on runoff, and that of a decreasing root depth on soil moisture (*i.e.*, due to decreasing depth of the soil profile and, thus, decreasing water storage capacity).

Figure 10. (**a**,**b**) Percent change and (**c**,**d**) first order sensitivity index (FOSI) for runoff (**left**) and soil moisture (**right**) for Senegal.
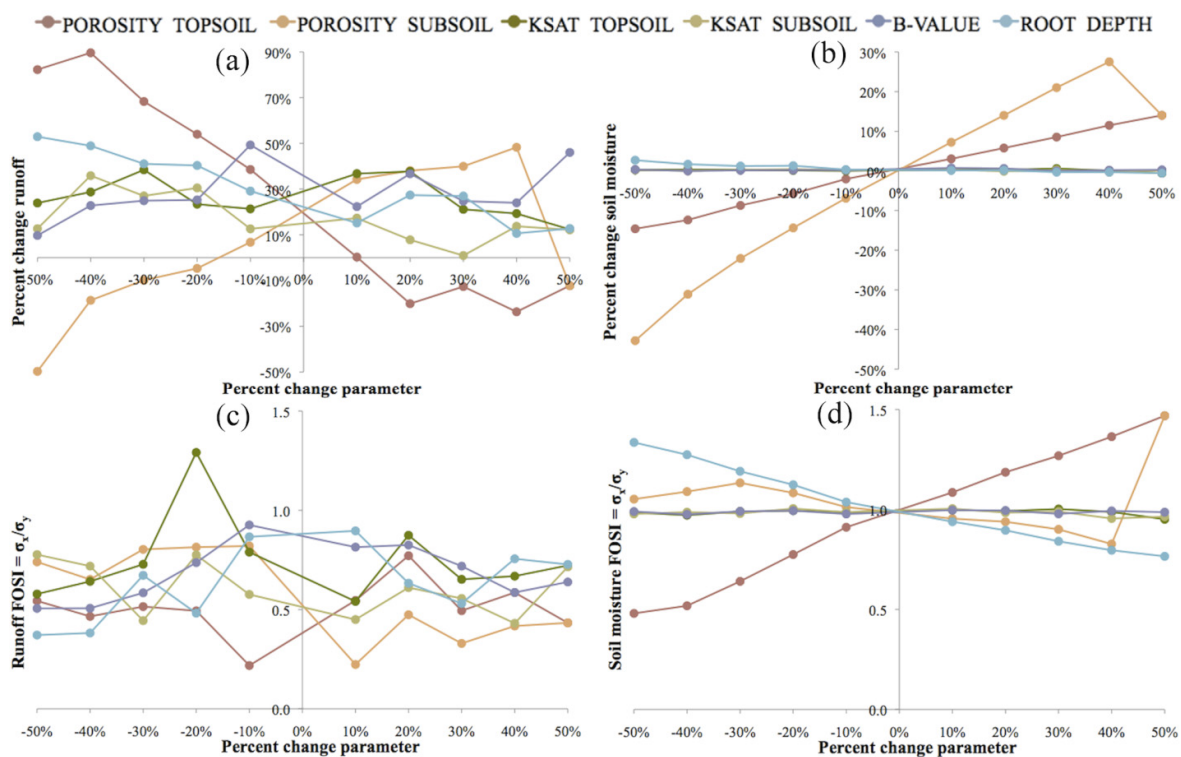
It is worth noting that changes in K_{sat} and the *b*-value do not induce substantial changes in soil moisture (Figures 9 and 10). As saturated hydraulic conductivity is only crudely approximated through soil textural information, K_{sat} values can vary greatly for sandy *versus* clayey soils. Thus, this shows that DryMOD is more robust for assessing soil moisture conditions than runoff and both runoff and soil moisture calculations depend on the realistic characterization of topsoil hydraulic properties through reliable soil parameterization.

In summary, the sensitivity analysis highlights the importance of soil parameterization to water balance modeling. The parameterization here was carried out on the basis of information derived from the 1-km spatial resolution HWSD database and information derived from the 1-km AVHRR-based land-cover dataset with reference values for root depth. However, spatial patterns relevant to the boundaries of soil mapping units at spatial scales coarser than 1-km were observed in the soil moisture maps. This suggests that soil parameterization at better spatial resolutions is advisable for more accurate derivation of the runoff and soil moisture components in water balance modeling.

5. Conclusions

This study presented and evaluated a new dynamic water balance model, DryMOD, which benefits from a novel means for spatial disaggregation and intensity correction of hourly rainfall at 1-km spatial resolution derived from Tropical Rainfall Measuring Mission (TRMM) datasets. Model performance was evaluated for two pilot catchments in Tunisia and Senegal through sensitivity analysis using the non-corrected and corrected for fractional cover of rainfall (FCR) TRMM-based rainfall forcing.

The results from model application to the study catchments in Tunisia and Senegal confirm the need for intensity correction and spatial disaggregation of the TRMM 3B42-based data implemented in DryMOD, which allows for hourly-based rainfall simulation and estimation of runoff and soil moisture at 1-km spatial resolution. Specifically, the model applications demonstrated that using the non-corrected TRMM based data fails to simulate realistic rainfall intensities and monthly totals as represented in the 1-km TRMM 2B31 climatology. While the annual average of mean monthly rainfall was up to 80 mm in Tunisia and 160 mm in Senegal in the TRMM 2B31-based dataset, the use of non-corrected TRMM 3B42 time series only generated annual average rainfall of up to 15 and 20 mm, respectively. This suggested that realistic hydrological fluxes such as runoff and soil moisture cannot easily be derived from TRMM 3B42 data. Indeed, simulated mean monthly runoff with the non-corrected dataset was below 0.2 mm for Tunisia and below 1.7 mm for Senegal, while using the FCR-corrected time series were used as the rainfall forcing in DryMOD resulted in mean monthly runoff of up to 26.5 and 54.9 mm, respectively. When the FCR-corrected dataset was used as the rainfall forcing for DryMOD, simulated mean soil moisture ranged between 0.07 and 0.30 $m^3 \cdot water \cdot m^{-3}$ soil for Tunisia and between 0.07 and 0.25 $m^3 \cdot water \cdot m^{-3}$ soil for Senegal with pronounced spatial patterns of key soil hydraulic properties such as K_{sat}.

As runoff in drylands is generated by high-intensity events with localized spatial extent, correction of rainfall intensities for the fractional cover of rainfall is required for realistic hydrological modeling. The analysis of runoff generating intensities showed that using the non-corrected TRMM based dataset fails to produce rainfall intensities higher than 7.19 $mm \cdot h^{-1}$ and 5 $mm \cdot h^{-1}$, while using the FCR-corrected dataset resulted in runoff generating intensities of up to 230 $mm \cdot h^{-1}$ and 40 $mm \cdot h^{-1}$ for the locations selected in Tunisia and Senegal, respectively. Although rainfall intensity data were not available for direct validation, previous work reported that 50% of rainfall in similar regions reaches the surface with intensities higher than 27 $mm \cdot h^{-1}$ and 32 $mm \cdot h^{-1}$. Additionally, our results indicated that 95% of rainfall intensities above 14.38 $mm \cdot h^{-1}$ and 95% of rainfall intensities above 5 $mm \cdot h^{-1}$ generated runoff in the selected 1-km pixel in the Tunisia and Senegal catchments, respectively. The results from the sensitivity analysis of runoff and soil moisture to six soil parameters

showed that for both pilot study catchments the greatest changes in runoff and soil moisture are in response to changes in the topsoil and subsoil porosities parameterization in DryMOD. Additionally, runoff and soil moisture showed sensitivity to changes in saturated hydraulic conductivity and root depth with most marked effects of root depth decrease below 2.5 m as it limits the soil depth and, thus, soil water storage capacity, and promotes saturation overland flow.

The following conclusions can be drawn from the analyses presented here:

- Improved realism of rainfall simulation allows for realistic estimation of the runoff ratio and help to identify runoff-generating areas in both study regions, representing differing dryland conditions in the belts north and south of the Sahara. Analysis of the runoff response to rainfall shows seasonal variability and provides information potentially useful for planning of water harvesting activities in the study regions.
- The sensitivity analysis revealed that changes in porosity of the topsoil and subsoil exert the maximum changes in runoff and soil moisture. This highlights the importance of soil parameterization through better information on soil properties at the regional-scale where detailed maps of hydrological fluxes are important for optimal planning of agricultural activities.

Acknowledgments

Conflicts of Interest

The authors declare no conflict of interest.

References

1. Cudennec, C.; Leduc, C.; Koutsoyiannis, D. Dryland hydrology in Mediterranean regions—A review. *Hydrol. Sci. J.* **2007**, *52*, 1077–1087.
2. Bolle, H.J.; Andre, J.C.; Arrue, J.L.; Barth, H.K.; Bessemoulin, P.; Brasa, A.; DeBruin, H.A.R.; Cruces, J.; Dugdale, G.; Engman, *etc.* EFEDA: European field experiment in a desertification threatened area. *Ann. Geophys.* **1993**, *11*, 173–189.
3. Helldén, U. Case Studies of Desertification Monitoring: A Discussion of EU Initiatives. In Proceedings of Local & Regional Desertification Indicators in a Global Perspective: AIDCCD-Active Exchange of Experience on Indicators and Development of Prespectives in the Context of UNCCD, Beijing, China, 16–18 May 2005.
4. Leemans, R.; Kleidon, A. Regional and Global Assessment of the Dimensions of Desertification. In *Global Desertification: Do Humans Cause Deserts*; Reynolds, J.F., Stafford Smith, D.M., Eds.; Dahlem University Press: Berlin, Germany, 2002; pp. 215–232.

5. Deus, D.; Gloaguen, R.; Krause, P. Water balance modeling in a semi-arid environment with limited *in situ* data using remote sensing in Lake Manyara, East African Rift, Tanzania. *Remote Sens.* **2013**, *5*, 1651–1680.

6. DeSurvey-IP. *DeSurvey: A Surveillance System for Assessing and Monitoring Desertification*. Available online: http://www.noveltis.com/desurvey (accessed on 3 December 2013).

7. Tarnavsky, E.; Mulligan, M.; Husak, G. Spatial disaggregation and intensity correction of TRMM-based rainfall time series for hydrological applications in dryland catchments. *Hydrol. Sci. J.* **2012**, *57*, 248–264.

8. Blöschl, G.; Sivapalan, M. Scale Issues in Hydrological Modelling: A Review. In *Scale Issues in Hydrological Modelling*; Kalma, J.D., Sivapalan, M., Eds.; Wiley: Chichester, UK, 1995.

9. Michaud, J.; Sorooshian, S. Comparison of simple *versus* complex distributed runoff models on a midsized semiarid watershed. *Water Resour. Res.* **1994**, *30*, 593–605.

10. Wheater, H. Hydrological Processes in Arid and Semi Arid Areas. In *Hydrology of Wadi Systems: IHP Regional Network on Wadi Hydrology in the Arab Region*; Wheater, H., Al-Weshah, R.A., Eds.; UNESCO International Hydrological Programme: Paris, France, 2002.

11. Al-Weshah, R.A. Rainfall-Runoff Analysis and Modelling in Wadi Systems. In *Hydrology of Wadi Systems: IHP Regional Network on Wadi Hydrology in the Arab Region*; Wheater, H., Al-Weshah, R.A., Eds.; UNESCO International Hydrological Programme: Paris, France, 2002.

12. Wesseling, C.G.; van Deursen, W.P.A.; de Wit, M. Rhine Basin. In *Third Joint European Conference Exhibition on Geographical Information*; Hodgson, S., Rumor, M., Harts, J.J., Eds.; IOS Press: Amsterdam, The Netherlands, 1997; pp. 487–496.

13. Mulligan, M. Global Gridded 1 km TRMM Rainfall Climatology and Derivatives. Version 1.0. Available online: http://geodata.policysupport.org/2b31climatology (accessed on 17 October 2013).

14. Mulligan, M. Three-Hourly Rainfall Time Series (from TRMM 3B42). Available online: http://geodata.policysupport.org/rainfall-timeseries (accessed on 17 October 2013).

15. Sharma, K.D.; Murthy, J.S.R. A practical approach to rainfall-runoff modelling in arid zone drainage basins. *Hydrol. Sci. J.* **1998**, *43*, 331–348.

16. CGIAR-CSI CGIAR-CSI SRTM 90m DEM Digital Elevation Database, Version 3.0. Available online: http://srtm.csi.cgiar.org (accessed on 17 October 2013).

17. Hlaoui, Z. Les Fortes Pluies Journalieres. In *Atlas de L'Eau en Tunisie*; Henia, L., Ed.; Université de Tunis: Tunis, Tunisia, 2008.

18. Ouessar, M. Watershed of Zeuss-Koutine in Médenine, Tunisia: Overview and Assessment Methodology. In *International Workshop on "Combating Desertification: Sustainable Management of Marginal Drylands (SUMAMAD)"*; UNU-UNSCO-ICARDA and Institut des Régions Arides (IRA): Shiraz, Islamic Republic of Iran, 2003; pp. 94–99.

19. Sagna, P. Charactéristiques Climatiques. In *Atlas du Sénégal*; Yahmed, D.B., Ed.; Les Éditions J.A.: Paris, France, 2007.

20. Kane, A.; Fall, A.N. Géologie et hydrogéologie. In *Atlas du Sénégal*; Yahmed, D.B., Ed.; Les Éditions J.A.: Paris, France, 2007.

21. NASA-GSFC TRMM Product Level 2B Combined (PR, TMI) Rainfall Profile: TRMM 2B31. Available online: http://disc.sci.gsfc.nasa.gov/precipitation/documentation/TRMM_README/ TRMM_2B31_readme.shtml (accessed on 17 October 2013).

22. NASA-GSFC TRMM and Other Satellites Precipitation Product. Available online: http://disc.gsfc.nasa.gov/precipitation/documentation/TRMM_README/TRMM_3B42_readme.s html (accessed on 17 October 2013).

23. FAO/IIASA/ISRIC/ISS-CAS/JRC. *Harmonized World Soil Database*; FAO: Rome, Italy, IIASA: Laxenburg, Austria, 2008; p. 37.

24. Mulligan, M. *Modelling the Hydrology of Vegetation Competition in a Degraded Semiarid Environment*; King's College London: London, UK, 1996.

25. Tranter, G.; Minasny, B.; Mcbratney, a.B.; Murphy, B.; Mckenzie, N.J.; Grundy, M.; Brough, D. Building and testing conceptual and empirical models for predicting soil bulk density. *Soil Use Manag.* **2007**, *23*, 437–443.

26. Hansen, M.; Defries, R.; Townshend, J.R.G.; Sohlberg, R. Global land cover classification at 1 km resolution using a decision tree classifier. *Int. J. Remote Sens.* **2000**, *21*, 1331–1365.

27. Zeng, X. Global vegetation root distribution for land modeling. *J. Hydrometeorol.* **2001**, *2*, 525–530.

28. Campbell, G.S. *Soil Physics with BASIC: Transport Models for Soil-Plant Systems*; Elsevier: Amsterdam, The Netherlands, 1985.

29. Thornthwaite, C.W. An approach toward a rational classication of climate. *Geogr. Rev.* **1948**, *38*, 55–94.

30. Palmer, W.C.; Havens, A.V. A graphical technique for determining evapotranspiration by the thornthwaite method. *Mon. Wea. Rev.* **1958**, *86*, 123–128.

31. Palmer, W.C. *Meteorological Drought*; US Weather Bureau: Washington, DC, USA, 1965; p. 58.

32. Mather, J.R.; Ambroziak, R.A. A search for understanding potential evapotranspiration. *Geogr. Rev.* **1986**, *76*, 355–370.

33. Iqbal, M. *Sun-Earth Astronomical Relationships: An Introduction to Solar Radiation*; Academic Press: London, UK, 1983.

34. Hijmans, R.J.; Cameron, S.E.; Parra, J.L.; Jones, P.G.; Jarvis, A. Very high resolution interpolated climate surfaces for global land areas. *Int. J. Climatol.* **2005**, *25*, 1965–1978.

35. Packer, R.W.; Sangal, B.P. The heat and water balance of southern Ontario according to the budyko method. *Can. Geogr.* **1971**, *XV*, 262–286.

36. Dyck, S. Overview on the Present Status of the Concepts of Water Balance Models. In *New Approaches in Water Balance Computation*; International Association of Hydrological Sciences (IAHS): Hamburg, Germany, 1983; pp. 3–19.

37. Xu, C.; Singh, V.P. A review on monthly water balance models for water resources investigations. *Water Resour. Manag.* **1998**, *12*, 31–50.

38. Hendrickx, M.H.; Phillips, F.M.; Harrison, B.J. Water Flow Processes in Arid and Semi-Arid Zones. In *Understanding Water in a Dry Environment*; Simmers, I., Ed.; A.A. Balkema Publishers: Lisse, The Netherlands, 2003.

39. Lange, J.; Leibundgut, C. Surface Runoff and Sediment Dynamics in Arid and Semi-Arid Regions. In *Understanding Water in a Dry Environment*; Simmers, I., Ed.; A.A. Balkema Publishers: Lisse, The Netherlands, 2003.

40. Akan, O.A. *Urban Stormwater Hydrology*: *A Guide to Engineering Calculations*; Technomic Publishing: Lancaster, PA, USA, 1993; p. 268.

41. Smith, R.E.; Goodrich, D.C. Rainfall Excess Overland Flow. In *Encyclopedia of Hydrologocal Sciences*; Anderson, M.G., Ed.; John Wiley & Sons, Ltd.: London, UK, 2005.

42. Warner, T.T. The Climates of the World Deserts. In *Desert Meteorology*; Cambridge University Press: Cambridge, UK, 2008; pp. 63–158.

43. Veihe, A.; Quinton, J. Sensitivity analysis of EUROSEM using Monte Carlo simulation I: Hydrological, soil and vegetation parameters. *Hydrol. Process.* **2000**, *14*, 915–926.

44. Saltelli, A.; Tarantola, S.; Campolongo, F.; Ratto, M. Methods based on Decomposing the Variance of the Output. In *Sensitivity Analysis in Practice*: *A Guide to Assessing Scientific Models*; John Wiley & Sons, Ltd.: Chichester, UK, 2004; p. 216.

45. Wainwright, J.; Mulligan, M.; Thornes, J. Plants and Water in Drylands. In *Eco-Hydrology: Plants and Water in Terrestrial and Aquatic Environments*; Baird, A.J., Wilby, R.L., Eds.; Routledge Physical Environment Series: London, UK, 1999; pp. 78–126.

46. Tabor, J.A. Improving crop yields in the Sahel by means of water-harvesting. *J. Arid Environ.* **1995**, *30*, 83–106.

47. Noy-Meir, I. Desert ecosystems: Environment and producers. *Annu. Rev. Ecol. Syst.* **1973**, *4*, 25–51.

48. Ceballos, A.; Martines-Fernandes, J.; Santos, F.; Alonso, P. Soil-water behaviour of sandy soils under semi-arid conditions in the Duero Basin (Spain). *J. Arid Environ.* **2002**, *51*, 501–519.

49. Twomlow, S.J.; Bruneau, P.M.C. The influence of tillage on semi-arid soil-water regimes in Zimbabwe. *Geoderma* **2000**, *95*, 33–51.

50. Balme, M.; Vischel, T.; Lebel, T.; Peugeot, C.; Galle, S. Assessing the water balance in the Sahel: Impact of small scale rainfall variability on runoff Part 1: Rainfall variability analysis. *J. Hydrol.* **2006**, *331*, 336–348.

51. Whittaker, J. Generating gamma and beta random variables with non-integral shape parameters. *Appl. Stat.* **1974**, *23*, 210–214.

52. Henia, L.; Benzarti, Z. Variabilite des Totaux Pluviometriques Annuels. In *Atlas de L'Eau en Tunisie*; Henia, L., Ed.; Université de Tunis: Tunis, Tunisia, 2008.

53. Global Gridded Surfaces of Selected Soil Characteristics (IGBP-DIS). Available online: http://daac.ornl.gov/ (accessed on 17 October 2013).